Journal of Alloys and Compounds 508 (2010) 426–432

Contents lists available at ScienceDirect

Journal of Alloys and Compounds

journal homepage: www.elsevier.com/locate/jallcom

Structural characterization and related properties of the stearate anions intercalated Ni–Al hydrotalcite-like compound prepared by the microwave crystallization

Lili Wang, Bin Li*, Chunxia Chen, Lina Jia

Department of Chemistry, College of Science, Northeast Forestry University, No. 26, Hexing Road, Harbin 150040, PR China

ARTICLE INFO

Article history:
Received 24 May 2010
Received in revised form 22 August 2010
Accepted 24 August 2010

Keywords:
Hydrotalcite-like compound
Microwave radiation
Thermal stability
X-ray diffraction

ABSTRACT

The stearate anions intercalated Ni–Al hydrotalcite-like compounds were prepared by a coprecipitation method coupled with the microwave-hydrothermal treatment. Their structures were characterized using FT-IR, XRD, contact angle, SEM, TEM and thermal analysis. The XRD results indicate that the interlayer anions of the microwave radiation samples have better order and stronger electrostatic interactions with hydroxyl layers than those of the conventional aging 12 h samples, the crystallinity of stearate anions intercalated Ni–Al hydrotalcite-like compounds can be rapidly enhanced in a short period of microwave treatment, and the stearate anions arrange in the form of a monolayer in the interlayer space for all samples. The morphology analysis results show that all samples consist of irregular and very thin platelets, while the crystals size of microwave treated samples was obviously smaller than that of the conventional aged samples. Based on the contact angle results, the surfaces of all samples show the hydrophobic property. This is due to the intercalation of stearate anions. The thermal analysis results point out that the sample obtained from microwave radiation 60 min possesses the best thermal stability. The rapid synthesis method explored in this paper is a promising method for studying other anionic surfactant intercalated HTLc.

© 2010 Elsevier B.V. All rights reserved.

1. Introduction

Hydrotalcite-like compounds (HTLcs), which are referred to as layered double hydroxides (LDHs) or anionic clays, are a large class of inorganic materials. The general formula of HTLc is written as $M^{2+}_{1-x}M^{3+}_{x}(OH)_2]^{x+}[A^{n-}]_{x/n} \cdot mH_2O$, where M^{2+} and M^{3+} are divalent and trivalent cations that occupy octahedral positions in the hydroxide layers, A^{n-} is an interlayer anion and x is defined as the $M^{3+}/(M^{2+}+M^{3+})$ molar ratio. The nature of layer metal ions can be changed in a wide possible selection range and the interlayer anion can be also chosen among inorganic or organic species. Therefore, HTLc have been extensively studied as catalysts, anionic exchangers, sorbents, additives, corrosion resistance film and precursor [1–8]. Especially in recent years, in order to improve the compatibility between polymers matrix and inorganic HTLc, the anionic surfactants modified-HTLc nanocomposites have attracted much interest of researchers [9–11]. It is worth emphasizing that the nano-scale anionic surfactants modified-HTLc can dramatically enhance mechanical performance, thermal stability and flame retardance of polymer/HTLc composites in comparison with the conventional polymer/inorganic composites with micro-scale and without organically modified fillers [12–14]. Therefore, the preparation of the anionic surfactants modified-HTLc with a good degree of crystallinity and high efficiency is crucial to the practical application.

In general, to obtain well-crystallized samples, most of the anionic surfactants modified-HTLc composites are synthesized by the coprecipitation with hydrothermal aging and the anion exchange techniques, and the reaction time needs from several hours to a few days [15–19]. It is well known, however, that the prolonged reaction time leads to the increase of crystal sizes. In recent years, the microwave technique has been considered to overcome the above shortcomings [20,21]. The important characteristic of microwave heating is its volumetric effect which results in a much more uniform distribution of heat [22–24]. Microwave heating is the transfer of electromagnetic energy to thermal energy and is energy conversion, rather than heat transfer [25–27]. Therefore, it permits to achieve rapid and uniform heating of materials. Nowadays, the microwave technique has been applied to the synthesis of modified-HTLc and unmodified-HTLc compounds [28–30]. However, the synthesis study on the stearate anions intercalated Ni–Al HTLc nanocomposite under the microwave radiation treatment can seldom be found in the literature.

This paper aims to explore a rapid synthesis method based on the microwave radiation crystallization, for obtaining the stearate anions intercalated Ni–Al HTLc samples. The influence of

* Corresponding author. Fax: +86 451 8219 1571.
E-mail addresses: liliwangsh@gmail.com (L. Wang), libinzh62@163.com (B. Li).

0925-8388/$ – see front matter © 2010 Elsevier B.V. All rights reserved.
doi:10.1016/j.jallcom.2010.08.080

Table 1
Chemical formulae, d_{003}, d_{006}, cell parameters (a, c), particle size (D), Δd and Gap for all intercalated samples.

Sample	Chemical formulae	d_{003} (nm)	d_{006} (nm)	a (nm)	c (nm)	Δd (Å)[a]	Gap (Å)[b]	D_{003} (nm)
HT12h	$Ni_{2.73}Al(OH)_{7.86}(C_{18}H_{35}O_2)_{0.45}(CO_3)_{0.07}(H_2O)_{2.50}$	3.740	1.512	0.302	10.15	32.60	6.32	12.78
HTN12h	$Ni_{2.97}Al(OH)_{8.58}(C_{18}H_{35}O_2)_{0.76}(CO_3)_{0.06}(H_2O)_{2.94}$	3.269	1.506	0.302	9.422	27.89	1.61	13.81
MWN10m	$Ni_{2.83}Al(OH)_{8.11}(C_{18}H_{35}O_2)_{0.44}(CO_3)_{0.06}(H_2O)_{5.56}$	3.199	1.504	0.302	9.311	27.19	0.91	9.81
MWN30m	$Ni_{2.93}Al(OH)_{8.11}(C_{18}H_{35}O_2)_{0.65}(CO_3)_{0.05}(H_2O)_{3.18}$	3.197	1.500	0.302	9.296	27.17	0.89	10.49
MWN60m	$Ni_{2.94}Al(OH)_{8.00}(C_{18}H_{35}O_2)_{0.86}(CO_3)_{0.06}(H_2O)_{3.75}$	3.152	1.496	0.302	9.216	26.72	0.44	15.66
MWN90m	$Ni_{2.89}Al(OH)_{8.10}(C_{18}H_{35}O_2)_{0.57}(CO_3)_{0.05}(H_2O)_{3.11}$	3.166	1.498	0.304	9.243	26.86	0.58	16.90

[a] The interlayer gallery height: $\Delta d = d_{003} - 4.8$ Å.
[b] Gap = Δd – the length of stearate anion (26.28 Å).

microwave radiation and N_2 protection condition on the nature of the interlayer anions, the crystallinity, the particle morphology, the thermal stability and the hydrophobicity of intercalation compound was investigated.

2. Experimental

For all preparations, nickel nitrate, aluminium nitrate, sodium hydroxide and sodium stearate were of the analytical grade.

Intercalation of stearate anions into the Ni–Al HTLc interlayer was implemented by the coprecipitate technique with microwave-hydrothermal crystallization. The pH of the 300 ml aqueous solution containing $C_{17}H_{35}COONa$ (0.16 M), $Ni(NO_3)_2$ and $Al(NO_3)_3$ ($[Ni^{2+}] = 0.75$ M and $[Al^{3+}] = 0.25$ M) was adjusted to 10 using 1 M NaOH aqueous solution with rapid stirring. For the comparing, the obtained slurry was submitted to different aging treatments: (a) the conventional hydrothermal treatment for 12 h at 70 °C under the conditions with strict N_2 protection and without N_2 protection. (b) The microwave-hydrothermal treatment for different periods of time (10, 30, 60 and 90 min) at 70 °C in a microwave oven (XH-300A, the maximum power of 1000 W and a frequency of 2.45 GHz). The temperature was controlled by the temperature feedback monitoring system with dual IR sensors. In all cases, the precipitates were washed with deionized water and ethanol until no nitrate and sodium were detected in the washing liquids, and then filtered. Finally, the samples were dried in an oven for 4 h at 70 °C.

The resulting samples were labeled by HTN12h and HT12h, where HT stands for the hydrothermal treatment, and N for N_2 protection. The samples submitted to the microwave (MW) radiation treatment were named as MWNt, where t (t = 10, 30, 60 and 90 min) stands for the microwave treatment time (minute).

The chemical analysis for Ni, Na and Al was carried out by the atomic absorption in the AAS-986 apparatus. The contents of C, N and H were determined using Leco CHNS-932. All samples were characterized by the powder X-ray diffraction (XRD) using D/MAX 2200 diffractometer with $\lambda = 1.5406$ Å for angle $2\theta = 2$–75°. Data were collected at the rate of 4°/min and step of 0.02° with Cu Kα irradiation operated at 40 kV and 45 mA. Infrared (IR) spectra of samples were obtained using Nicolet FTIR360 spectrometer (KBr pellet method, 4 cm^{-1} resolution). Thermal analysis and the weight loss percentages of H_2O were carried out with a thermogravimetric analyzer (TGA pyris 1 from PerkinElmer) using a constant heating rate of 10 °C/min under nitrogen atmosphere from 50 to 800 °C. Morphology of the specimens was examined in HITACHI 1H-7650 transmission electron microscope (TEM) operated at an accelerating voltage of 100 kV. Scanning electron microscope (SEM) observations were carried out on FEI-Sirion with a field emission at 20 kV. The EDX analysis of samples was obtained by SEM equipped with the EDAX genesis X-ray energy-dispersive spectrometry system through a spectrum imaging technique. Contact angles (CA) were measured using JC2000A contact angle/interface tensile measurer. All samples were pressed into disks with a diameter of 11 mm. Each disk was dripped by 10 μL of deionized water, and the observation of all water drops maintains for 15 s. Each sample repeats the experiment 10 times in the measurement.

3. Results and discussion

3.1. Element chemical analysis

The compositions of all intercalated samples were obtained using AAS, CHN and TGA characterization techniques. These results can determine the chemical formulae of the conventional hydrothermal treatment and the microwave radiation treated samples, as summarized in Table 1. The observation shows that the stearate anions are the main interlayer anions in all the samples. The measured atomic molar ratio of Ni/Al is approximately the ratio of the metal cations in the initial solution, except for HT12h, whose ratio is lower than that of other samples. The contents of N and Na elements are less than 0.03%, which indicates that the nitrate anions and sodium stearate moleculars are absent in all samples. In addition, a small amount of carbonates can coexist in the interlayer space based on the compositional analysis, especially for the HT12h sample without N_2 protection.

3.2. FT-IR characterization

The IR technique has been commonly used to identify the nature of the interlayer anions and the presence of impurity in non-crystalline phases. The FT-IR spectra of six intercalated samples and the sodium stearate recorded at room temperature are presented in Fig. 1(a)–(g). In all cases, Fig. 1(a)–(f) shows that the broad and intense absorption bands between 3700 and 3100 cm^{-1} centered at about 3460 cm^{-1} are due to the O–H stretching vibrations of layer hydroxyl groups and interlayer water molecules in the stearate anions intercalated samples. The weak shoulder at 2971 cm^{-1} and two strong peaks at 2917 and 2850 cm^{-1} correspond to C–H stretching vibration of stearate anions. In addition, a very weak shoulder at about 1365 cm^{-1} appeared in all intercalated samples demonstrates the presence of very small amounts of interlayer carbonate ions. The reason is due to the contamination from the absorption of atmospheric CO_2 under high pH solution during washing. In fact, this contamination is difficult to be avoided [31]. Namely, the stearate anions and a very small amount carbonates were embedded in the interlayer space of intercalated samples. This result is in agreement with the element chemical analysis. The bands near 1635 cm^{-1} can be assigned to the bending vibration of interlayer water molecules in the intercalated samples [32]. This characteristic band of MWN10m is relative intense. It indicates that MWN10m contains the more interlayer water than other intercalated sample. The sharp and intense characteristic absorption band at 1560 cm^{-1} is attributed to the antisymmetric stretching vibra-

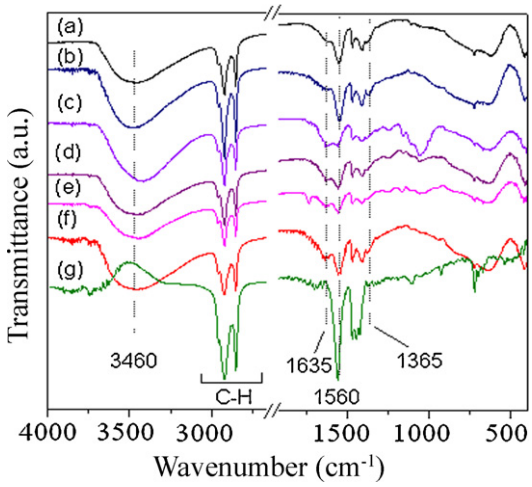

Fig. 1. FT-IR spectra of all intercalated samples and sodium stearate. (a): HT12h, (b): HTN12h, (c): MWN10m, (d): MWN30m, (e): MWN60m, (f): MWN90m and (g): sodium stearate.

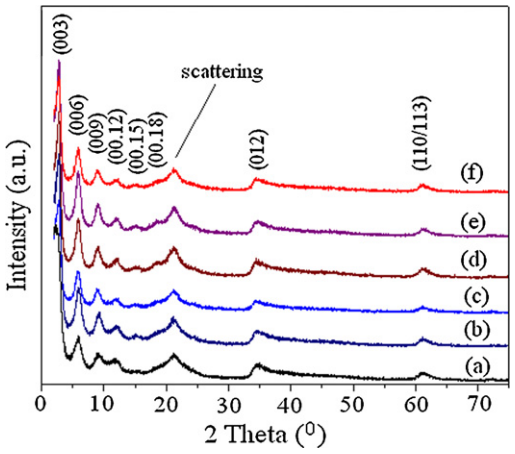

Fig. 2. X-ray diffraction patterns for six intercalated samples. (a): HT12h, (b): HTN12h, (c): MWN10m, (d): MWN30m, (e): MWN60m and (f): MWN90m.

tion of the carboxylate group [33,34]. Simultaneously, the peaks at 1467 and 1410 cm^{-1} correspond to the CH_2 scissoring and the symmetric stretching vibrations of the carboxylate group. The above three characteristic peaks of stearate anions also appear in all intercalated samples.

3.3. X-ray diffraction study

Fig. 2(a)–(f) shows the powder X-ray diffraction patterns of all six intercalated samples. All main diffraction peaks (0 0 3), (0 0 6), (0 0 9) and (0 0 12) were appeared in the very low angle due to the intercalation of $C_{17}H_{35}COO^-$ anions in the interlayers of Ni–Al HTLc, whether by the microwave radiation or the conventional heating treatment. These patterns are typical character of organo-HTLc composites [35]. Furthermore, the (1 1 0) and (1 1 3) diffraction peaks are overlapped together to form broad and non-symmetric lines. It demonstrates that HTLc contains large anions in the interlamellar region [20,36]. In addition, it should be also noted that a broad peak in the range of 20–23° corresponds to the scattering by the hydrocarbon chains [37]. This characteristic peak also confirms that stearate anions are intercalated into the Ni–Al HTLc interlayers.

A steady enhancement of the crystalline degree in the microwave radiation samples is observed as the (0 0 3), (0 0 6) and (0 0 9) diffraction lines become sharper and stronger when the radiation time is at between 10 and 60 min. Interestingly, the crystalline degree of MWN90m shows no continuous improvement when the radiation time is increased up to 90 min. In reverse, the intensity of all peaks is decreased. This character is similar to that of some compounds aged under a microwave-hydrothermal treatment which were attributed to the finite Ostwald ripening [38,39]. Therefore, the best crystallinity improvement was attained after 60 min microwave heating treatment for this series of intercalated samples.

From the positions of the peaks in the XRD patterns, the values of the lattice parameters a and c can be calculated according to a 3R packing of the layers [40,41]. The c parameter (namely three times the distance between the brucite-like layers) equals three times the value of $d_{(003)}$ or six times the value of $d_{(006)}$ if the peaks are sharp enough [42,43]. However, as the peaks are somewhat broad, the lattice parameter c can be calculated by averaging the (0 0 3) and (0 0 6) positions, according to the following equation [44–47]:

$$c = \left(\frac{3}{2}\right)[d_{(003)} + 2d_{(006)}] \quad (1)$$

The a parameter, namely the average cation–cation distance within the layers, has been calculated from the (1 1 0) reflection

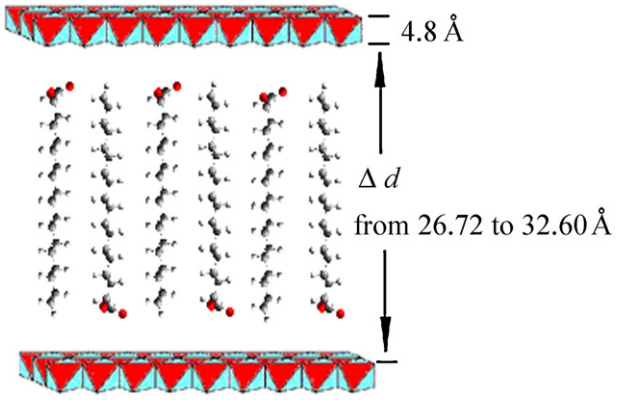

Fig. 3. Schematic arrangement of stearate anions with a monolayer in the interlayer for all intercalated samples.

according to the equation $a = 2d_{(110)}$. The crystallite sizes in c axis directions can be determined by using Scherrer formula [48–50]:

$$D = \frac{0.89\lambda}{B(\theta)\cos(\theta)} \quad (2)$$

where D is the crystallite size, λ is the wavelength of the radiation used, $B(\theta)$ is the full width at half maximum (FWHM) of the (0 0 3) diffraction peaks (rad.), and θ is the Bragg diffraction angle for each sample. The cell parameters (a, c) and particle size (D) of all samples are included in Table 1.

The parameter a depends on the chemical composition of the metal cations in the layers. The a values remain almost constant 0.302 nm except for MWN90m whose a value is 0.304 nm. These values are in good agreement with that of MgAl–LDH determined by XRD [51]. The reason is due to the similar radii of Ni^{2+} and Mg^{2+} (rMg^{2+} = 0.720, rNi^{2+} = 0.690 Å). The c values of HT12h and HTN12h are 10.15 and 9.422 nm, respectively. They are greater than other sets of samples by the microwave treatment. In addition, there is a steady decrease in the c parameter with the increase of microwave radiation time from 10 to 60 min as expected. However, when the microwave radiation time was further increased, the c value of MWN90m increased. This parameter is related to the electrostatic forces between the layers and the interlayer anions. Usually the

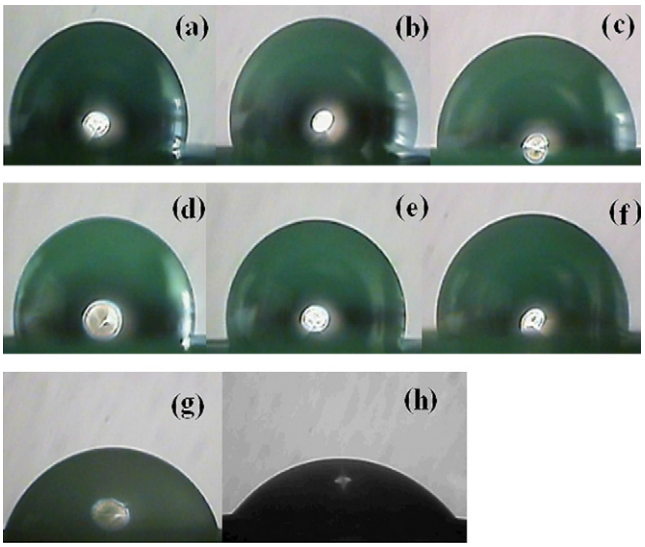

Fig. 4. Contact angle of all samples. (a): HT12h with CA 100°, (b): HTN12 h with CA 105°, (c): MWN10m with CA 95°, (d): MWN30m with CA 99°, (e): MWN60m with CA 102°, (f): MWN90m with CA 97°, (g): sodium stearate with CA 75° and (h): Ni–Al–CO_3 with CA 46°.

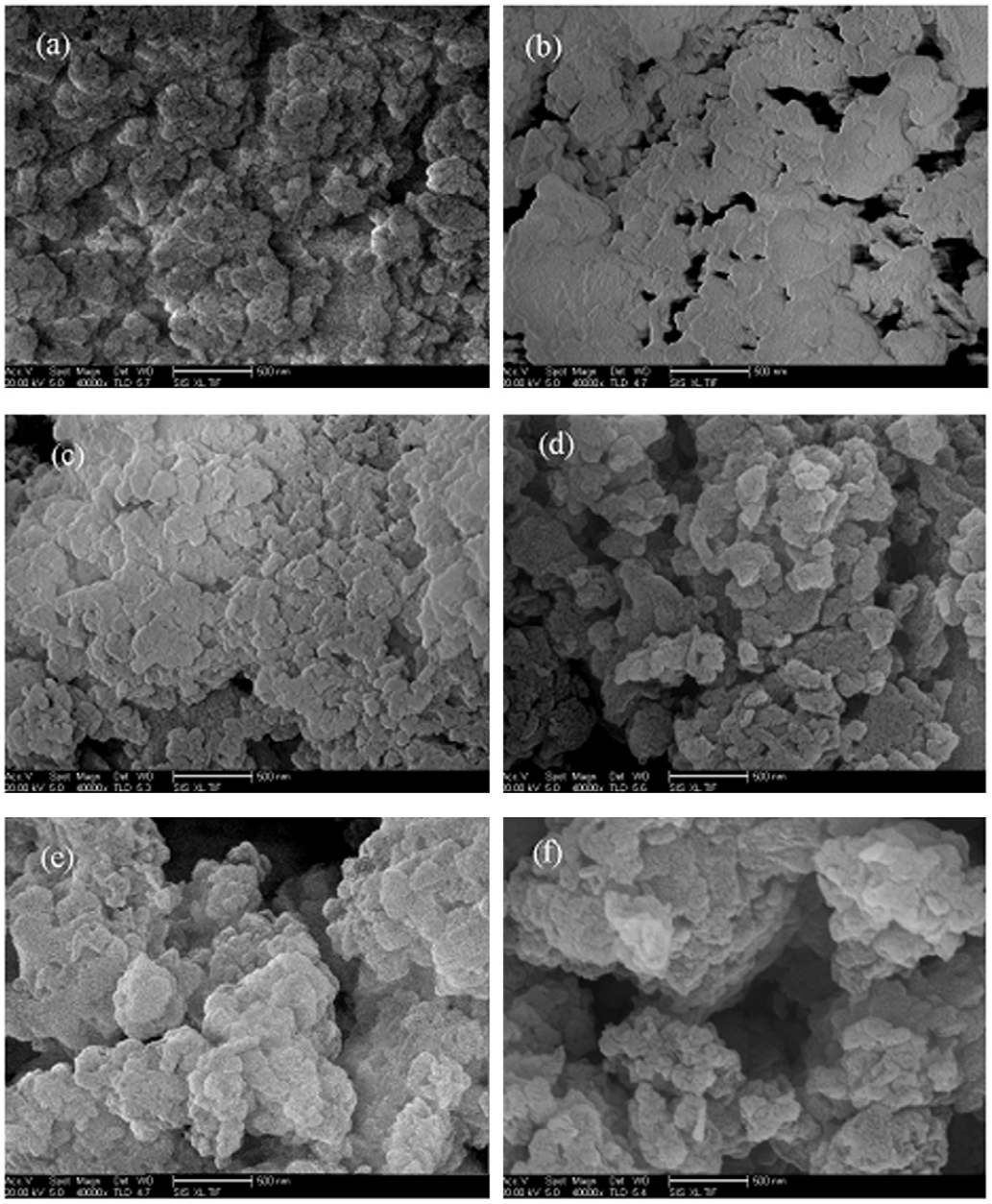

Fig. 5. SEM images of six intercalated samples. (a): HT12h, (b): HTN12h, (c): MWN10m, (d): MWN30m, (e): MWN60m and (f): MWN90m.

interlamellar region is well ordered and the electrostatic interactions between anionic species and hydroxyl layers become to be enhanced with the decrease of the *c* parameter [34,44]. Therefore, it can be concluded that the interlayer anions of the microwave radiation samples are well ordered and have stronger electrostatic interactions with hydroxyl layers in comparison with the conventional aging 12 h samples.

The layer spacing (d_{003}) decreased as the microwave time increased from 10 to 60 min. However, when the radiation time was further increased, the spacing of MWN90m increased and the basal reflection became weaker and broader. It is an indication of lower crystallinity [52]. The HT12h shows a lower crystallinity due to the weaker and broader diffraction peaks. Furthermore, its (0 0 3) diffraction peak 2θ angle (2.36°) is 0.5° lower than that of other samples (2.86°). It can be concluded that interlayer anions species of HT12h increased because there is no N_2 protection. It leads to a low ordering of interlayer anions. In addition, the intensity and the position of diffraction peaks for MWN30m are very close to that of the sample HTN12h. It means that the crystalline degrees are similar for the products MWN30m and HTN12h.

The crystallite sizes of all samples were calculated by the Scherrer equation [48–50]. A sustained increase of the particle size is observed during the microwave treatment. Further, a fast growth occurs at between 30 and 60 min. In all samples, the intercalation of the organic stearate anions leads to the expansion of the interlayer space in comparison with the values reported in the literature for the Ni–Al–carbonate HTLc (Ni:Al molar ratio = 3) [53]. According to the chain length of the myristic acid molecule $CH_3(CH_2)_{12}COOH$ (21.2 Å) [54] and the C–C distance in paraffins (1.27 Å) [55], the dimension of stearate anions is approximately 26.28 Å. Taking into account that the thickness of a brucite-like layer is about 4.8 Å [56,57], so that the interlayer gallery height (Δd) ranges from 26.72 to 32.60 Å according to the equation: $d_{003} - 4.8$ Å for all intercalated samples [58]. Therefore, all samples exhibit the arrangement of a monolayer of stearate anions according to Δd values and the length of stearate anion (26.28 Å), as shown in Fig. 3. However, all

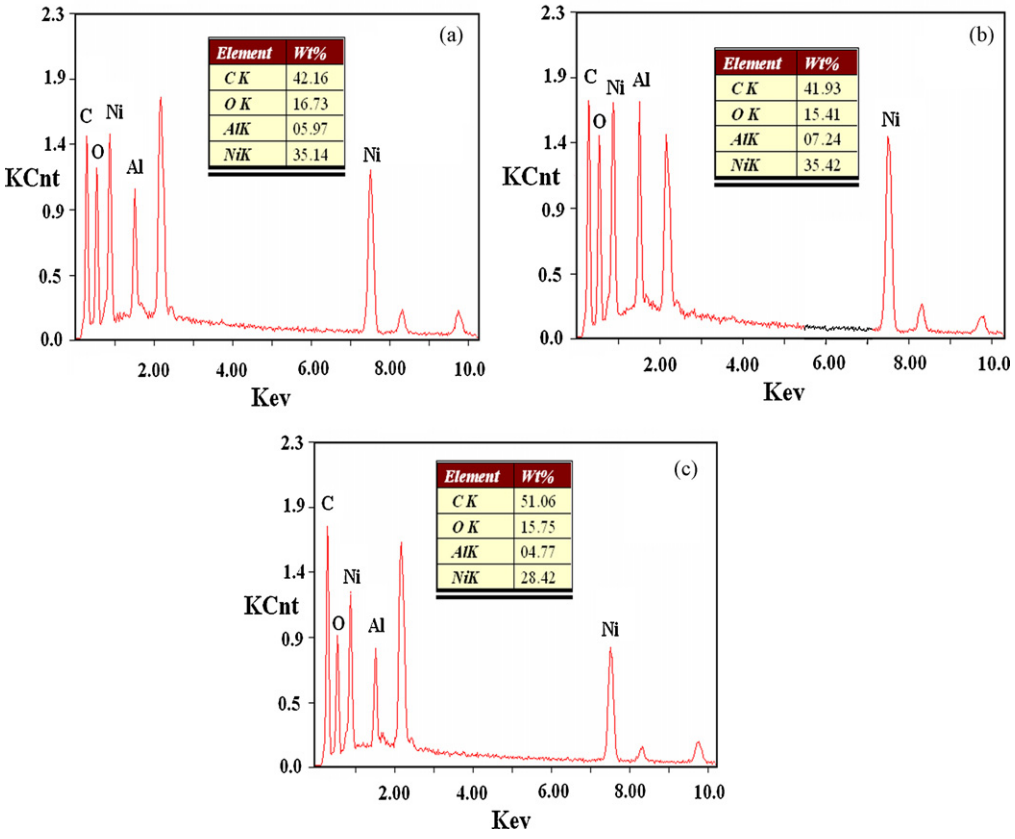

Fig. 6. EDX analysis of (a): HT12h, (b): MWN30m and (c): MWN90m.

Δd values are found to be larger than the length of the intercalated stearate anions. To account for these additional spaces, the gaps existing between the interlayer and organic ions were calculated by the equation: Δd – the length of stearate anion (26.28 Å) [59]. Furthermore, the Δd and the gap values of all intercalated samples are also listed in Table 1. The gap value (6.32 Å) of HT12h is greater than other intercalated samples. This result is mainly attributed to two potential reasons. Firstly, the important factor is that the electrostatic interaction between the brucite-like layer and the interlaminar stearate anions in HT12h is weaker than that in other samples [59]. The differences of gap values also indicate that the interlayer anions of the microwave radiation samples have stronger electrostatic interactions with hydroxyl layers than those of the conventional aging 12 h samples. This result is in agreement with the *c* value analysis. Secondly, the different arrangement of interlayer water molecules can also lead to the change of the gap value, as described by Arizaga et al. [58] and Wypych et al. [59].

3.4. Hydrophilic and hydrophobic analysis

In order to confirm the influence of stearate anions intercalation on the hydrophilic and the hydrophobic property of all samples, the contact angles were measured. Fig. 4 shows all images of the contact angles. The results show that the contact angle steadily increases from 95 to 102° when the microwave radiation time ranges from 10 to 60 min. However, the contact angle of MWN90m with microwave radiation 90 min decreases to 97°. In addition, the contact angles of all intercalated samples are larger than that of the pure sodium stearate (75°) and our previous prepared Ni–Al–CO_3 (46°). It indicates that the surfaces of all intercalated samples show the change from hydrophilicity to hydrophobicity due to the intercalation of stearate anions. Because the surface hydrophobic property of intercalated samples can be modified by controlling the microwave radiation time, the modified-HTLc nanocomposite of the different hydrophobic property can be prepared by different microwave radiation conditions.

3.5. The morphology analysis

SEM images of all intercalated samples were shown in Fig. 5(a)–(f). As seen from all SEM images, their surface morphology becomes lamellar plates and stacks parallelly to each other. Furthermore, HTN12h and MWN10m show more evident lamellar plate-like shape compared with other samples. Therefore, in order to obtain more fine morphology and particle size distribution, the TEM images of all intercalated samples are analyzed (not shown). The TEM micrograph was obtained by transferring a drop of suspension onto a grid. All images show irregular and very thin platelets oriented parallel to the grid surface. Moreover, the overlap phenomenon occurs among the platelets. It is due to that the particle–particle interactions are strong, especially for the microwave radiation samples. In addition, the particle sizes of all samples increased as the aging time was prolonged, and the particle size of microwave treated samples was smaller than that of the conventional aged samples.

Fig. 6(a)–(c) shows the EDX analysis of three samples HT12h, MWN30m and MWN90m, respectively. In all EDX figures, no N and Na elements were detected in the chemical composition. It excludes the existence of nitrates and sodium stearate moleculars. The above results are in good agreement with the elemental analysis results.

3.6. Thermal analysis

The nature of the interactions between host layers and guest anions can be investigated by the thermal analysis, and the thermal stability depends on the crystallinity degree of samples [60,61].

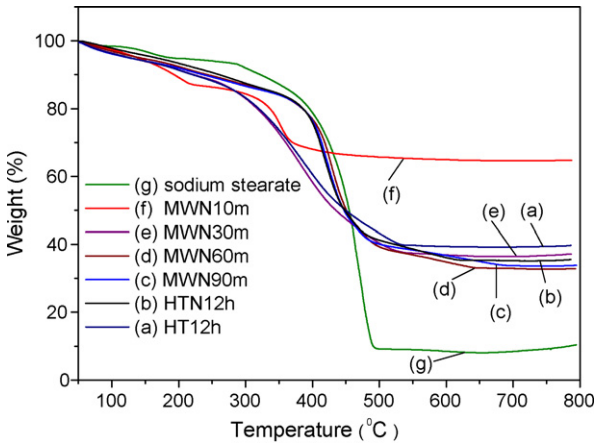

Fig. 7. TGA curves of sodium stearate and six intercalated samples. (a): HT12h, (b): HTN12h, (c): MWN90m, (d): MWN60m, (e): MWN30m, (f): MWN10m and (g): sodium stearate.

Figs. 7 and 8 show the TGA and DTG curves of sodium stearate and all intercalated samples.

TGA curves of all six intercalated samples show two weight loss stages. The first step in the range of 50–240 °C centered at 60 and 200 °C in the DTG curves are attributed to the removal of physisorbed water and interlayer water. The weight loss of MWN10m accounts for 18% of the initial weight of the sample at 240 °C. This weight loss is larger than the other five intercalated samples, of which weight losses are in the range 9–12% of the initial sample weight. With increasing the temperature, the second weight loss is completed by ~450 °C for MWN10m accounting for 34% of the initial sample weight. While the weight losses of the other five intercalated samples are completed by ~560 °C. They are in the range 61–64% of the initial samples weight, respectively. These weight losses can be attributed to the removal of both layer hydroxyls and interlayer anion groups.

However, the accurate change of thermal stability at the second weight loss stage shows obvious differences in the DTG curves for all six intercalated samples. For instance, MWN10m shows a symmetrical and sharp peak centered at 354 °C which is about 120 °C lower than the strong and sharp peaks centered at 464 and 475 °C of stearate anions. This result indicates that the interlayer anions of MWN10m contain a small amount of stearate anions and a large number of hydroxyls [62,63], which is in agreement with

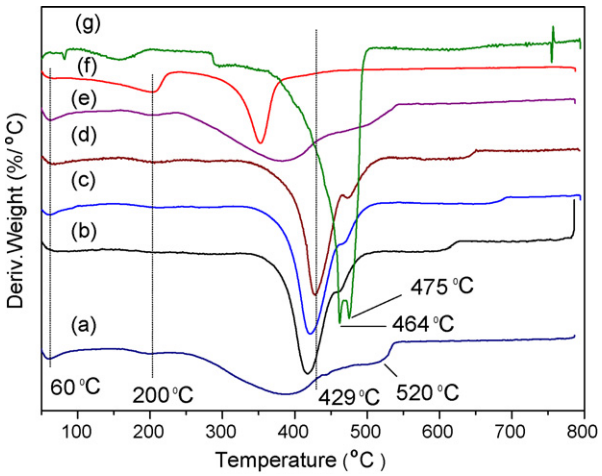

Fig. 8. DTG curves of sodium stearate and six intercalated samples. (a): HT12h, (b): HTN12h, (c): MWN90m, (d): MWN60m, (e): MWN30m, (f): MWN10m and (g): sodium stearate.

the IR spectra. MWN30m and HT12 h show similar broad peaks in the range of 240–540 °C centered at about 393 °C in the DTG curve. This result suggests that their interlayer anions are hydroxyls and $C_{18}H_{35}O^{2-}$ together. In addition, they show another weak shoulder peak at about 520 °C. This high decomposition temperature is due to the hydrogen bonding interactions between CO_3^{2-} and $C_{18}H_{35}O^{2-}$. However, a shift of the third sharp and strong peak of HTN12h towards higher temperatures at 417 °C with a weak shoulder peak at about 467 °C are observed in the DTG profile. Moreover, all peak shapes and positions of MWN60m and MWN90m are very similar to that of HTN12h. The third peaks of MWN60m and MWN90m move toward higher temperatures at 429 and 423 °C, respectively. And they also present a weak shoulder peak at about 475 and 472 °C, respectively. These peaks are due to the decomposition of all $C_{18}H_{35}O^{2-}$ in the interlayer. Note that the intensity of the interlayer water peak becomes weak as the aging time was prolonged. This fact also confirms that the intercalated amount of stearate anions was increased, since the hydrophobicity of $C_{18}H_{35}O^{2-}$ decreases the affinity with the interlayer water in comparison with the hydroxyl groups.

The above results indicate that both microwave radiation time and N_2 protection condition have important influences on the intercalation of stearate anions, and intercalation effect of $C_{18}H_{35}O^{2-}$ under microwave radiation 60 min is the best in all six samples. Thus, it can be concluded that the increase in crystallinity also affects the thermal stability of the samples. On the other hand, the thermal analysis also confirms that the intercalation of $C_{18}H_{35}O^{2-}$ anions into the interlayer of HTLc occurs both in coprecipitation stage and especially in the aging step.

4. Conclusions

In this paper, the anionic surfactant organic modified-Ni–Al HTLc with stearate anions was prepared by the coprecipitation. And the effects of two methods including the microwave radiation aging and the conventional hydrothermal treatment on the homogeneity and the crystallinity were comparatively investigated.

The chemical element composition and EDX analysis indicate that no nitrate anions and sodium stearate moleculars exist in all samples. The IR results show that the stearate anions and a very small amount of carbonates were embedded in the interlayer space of intercalated samples together. The XRD results illustrate that the sample of microwave radiation 60 min shows the best crystallinity. However, HT12h shows lower crystallinity and lower 2θ angle of basal plane (0 0 3) than other samples due to no N_2 protection. Finally, the thermal analysis results indicate that the enhancement of crystallinity improves the thermal stability of the samples. Furthermore, the intercalation of $C_{17}H_{35}COO^-$ anions into the interlayer of HTLc occurs in both coprecipitation process and the aging process, especially the latter.

Acknowledgements

The authors would like to express their thanks for the financial support from Technical Innovation Personnel Special Foundation of Harbin (No. 2008RFQXG012) and Youth Foundation of Northeast Forestry University (No. 09025).

References

[1] M. Mokhtar, S.N. Basahel, Y.O. Al-Angary, J. Alloys Compd. 493 (2010) 376–384.
[2] R. Marangoni, M. Bouhent, C. Taviot-Guého, F. Wypych, F. Leroux, J. Colloid Interface Sci. 333 (2009) 120–127.
[3] J.J. Yu, J. Cheng, C.Y. Ma, H.L. Wang, L.D. Li, Z.P. Hao, Z.P. Xu, J. Colloid Interface Sci. 333 (2009) 423–430.
[4] A. Das, F.R. Costa, U. Wagenknecht, G. Heinrich, Eur. Polym. J. 44 (2008) 3456–3465.

[5] M. Halma, K.A.D.F. Castro, V. Prévot, C. Forano, F. Wypych, S. Nakagaki, J. Mol. Catal. A: Chem. 310 (2009) 42–50.
[6] J. Wang, D. Li, X. Yu, X. Jing, M. Zhang, Z. Jiang, J. Alloys Compd. 494 (2010) 271–274.
[7] H. Liu, Q. Jiao, Y. Zhao, H. Li, C. Sun, X. Li, J. Alloys Compd. 496 (2010) 317–323.
[8] X. Xiang, G. Fan, J. Fan, F. Li, J. Alloys Compd. 499 (2010) 30–34.
[9] H. Peng, W.C. Tjiu, L. Shen, S. Huang, C. He, T. Liu, Compos. Sci. Technol. 69 (2009) 991–996.
[10] C.M. Nshuti, P. Songtipya, E. Manias, M.M.J. Gasco, J.M. Hossenlopp, C.A. Wilkie, Polym. Degrad. Stab. 94 (2009) 2042–2054.
[11] F. Kovanda, E. Jindová, K. Lang, P. Kubát, Sedláková Z., Appl. Clay Sci. 48 (2010) 260–270.
[12] Y. Shi, F. Chen, J. Yang, M. Zhong, Appl. Clay Sci., in press, doi:10.1016/j.clay.2010.07.007.
[13] M. Zhang, P. Ding, L. Du, B. Qu, Mater. Chem. Phys. 109 (2008) 206–211.
[14] C.M. Nshuti, P. Songtipya, E. Manias, M.M.J. Gasco, J.M. Hossenlopp, C.A. Wilkie, Polymer 50 (2009) 3564–3574.
[15] Z.P. Xu, P.S. Braterman, Appl. Clay Sci. 48 (2010) 235–242.
[16] B. Magagula, N. Nhlapo, W.W. Focke, Polym. Degrad. Stab. 94 (2009) 947–954.
[17] S. Lv, W. Zhou, H. Miao, W. Shi, Prog. Org. Coat. 65 (2009) 450–456.
[18] S.P. Lonkar, S. Therias, N. Caperaa, F. Leroux, J.L. Gardette, Eur. Polym. J. 46 (2010) 1456–1464.
[19] F.R. Costa, A. Leuteritz, U. Wagenknecht, M.A. Landwehr, D. Jehnichen, L. Haeussler, G. Heinrich, Appl. Clay Sci. 44 (2009) 7–14.
[20] M. Herrero, F.M. Labajos, V. Rives, Appl. Clay Sci. 42 (2009) 510–518.
[21] S. Beg, A.A. Alas, N.A.S.A. Areqi, J. Alloys Compd. 493 (2010) 299–304.
[22] E.T. Thostenson, T.W. Chou, Compos. Part A 30 (1999) 1055–1071.
[23] S. Farhadi, S. Sepahvand, J. Alloys Compd. 489 (2010) 586–591.
[24] A.M. Ibrahim, M.M. Abd El-Latif, M.M. Mahmoud, J. Alloys Compd. 506 (2010) 201–204.
[25] D.D. Upadhyaya, A. Ghosh, K.R. Gurumurthy, R. Prasad, Ceram. Int. 27 (2001) 415–418.
[26] C.T. Lee, F.S. Chen, C.H. Lu, J. Alloys Compd. 490 (2010) 407–411.
[27] M. Oghbaei, O. Mirzaee, J. Alloys Compd. 494 (2010) 175–189.
[28] M. Herrero, P. Benito, F.M. Labajos, V. Rives, Y.D. Zhu, G.C. Allen, J.M. Adams, J. Solid State Chem. 183 (2010) 1645–1651.
[29] P. Benito, M. Herrero, F.M. Labajos, V. Rives, Appl. Clay Sci. 48 (2010) 218–227.
[30] S. Cho, S.H. Jung, J.W. Jang, E. Oh, K.H. Lee, Cryst. Growth Des. 8 (2008) 4553–4558.
[31] L. Du, B. Qu, J. Mater. Chem. 16 (2006) 1549–1554.
[32] M. Herrero, P. Benito, F.M. Labajos, V. Rives, Catal. Today 128 (2007) 129–137.
[33] L. Zhang, Y. Lin, Z. Tuo, D.G. Evans, D. Li, J. Solid State Chem. 180 (2007) 1230–1235.
[34] P. Benito, F.M. Labajos, J. Rocha, V. Rives, Micropor. Mesopor. Mater. 94 (2006) 148–158.
[35] H. Zhang, X. Wen, Y. Wang, J. Solid State Chem. 180 (2007) 1636–1647.
[36] P. Benito, F.M. Labajos, L. Mafra, J. Rocha, V. Rives, J. Solid State Chem. 182 (2009) 18–26.
[37] Z.P. Xu, P.S. Braterman, J. Mater. Chem. 13 (2003) 268–273.
[38] P. Benito, M. Herrero, F.M. Labajos, V. Rives, C. Royo, N. Latorre, A. Monzon, Chem. Eng. J. 149 (2009) 455–462.
[39] P. Benito, I. Guinea, F.M. Labajos, J. Rocha, V. Rives, Micropor. Mesopor. Mater. 110 (2008) 292–302.
[40] H.S. Panda, R. Srivastava, D. Bahadur, Mater. Res. Bull. 43 (2008) 1448–1455.
[41] S. Britto, A.V. Radha, N. Ravishankar, P.V. Kamath, Solid State Sci. 9 (2007) 279–286.
[42] G. Hu, D. O'Hare, J. Am. Chem. Soc. 127 (2005) 17808–17813.
[43] L. Ren, J.S. Hu, L.J. Wan, C.L. Bai, Mater. Res. Bull. 42 (2007) 571–575.
[44] L.H. Su, X.G. Zhang, J. Power Sources 172 (2007) 999–1006.
[45] C. Jaubertie, M.J. Holgado, M.S. San Romn, V. Rives, Chem. Mater. 18 (2006) 3114–3121.
[46] F.M. Labajos, M.D. Sastre, R. Trujillano, V. Rives, J. Mater. Chem. 9 (1999) 1033–1039.
[47] M. Acro, P. Male, R. Trujillano, V. Rives, Chem. Mater. 11 (1999) 624–633.
[48] M.A. Pagano, C. Forano, J.P. Besse, J. Mater. Chem. 13 (2003) 1988–1993.
[49] A.R. Auxilio, P.C. Andrews, P.C. Junk, L. Spiccia, D. Neumann, W. Raverty, N. Vanderhoek, Polyhedron 26 (2007) 3479–3490.
[50] F. Li, X. Liu, Q. Yang, J. Liu, D.G. Evans, X. Duan, Mater. Res. Bull. 40 (2005) 1244–1255.
[51] Z.P. Xu, H.C. Zeng, J. Phys. Chem. B 105 (2001) 1743–1749.
[52] G.G.C. Arizaga, A.S. Mangrich, F. Wypych, J. Colloid Interface Sci. 320 (2008) 238–244.
[53] U. Costantino, M. Curini, F. Montanari, M. Nocchetti, O. Rosati, J. Mol. Catal. A: Chem. 195 (2003) 245–252.
[54] M. Borja, P.K. Dutta, J. Phys. Chem. 96 (1992) 5434–5444.
[55] M. Meyn, K. Beneke, G. Lagaly, Inorg. Chem. 32 (1993) 1209–1215.
[56] M. Jakupca, P.K. Dutta, Chem. Mater. 7 (1995) 989–994.
[57] T. Kwon, G.A. Tsigdinos, T.J. Pinnavaia, J. Am. Chem. Soc. 110 (1988) 3653–3654.
[58] G.G.C. Arizaga, A.S. Mangrich, J.E.F.C. Gardolinski, F. Wypych, J. Colloid Interface Sci. 320 (2008) 168–176.
[59] F. Wypych, G.G.C. Arizaga, J.E.F.C. Gardolinski, J. Colloid Interface Sci. 283 (2005) 130–138.
[60] S. Kannan, A. Narayanan, C.S. Swamy, J. Mater. Sci. 31 (1996) 2353–2360.
[61] S. Mohmel, I. Kurzawski, D. Uecker, D. Muller, W. Gebner, Cryst. Res. Technol. 37 (2002) 359–369.
[62] J.M. Fernandez, M.A. Ulibarri, F. Labajos, V. Rives, J. Mater. Chem. 8 (1998) 2507–2514.
[63] L. Hickey, J.T. Kloprogge, R.L. Frost, J. Mater. Sci. 35 (2000) 4347–4355.